Paper Number:
DOE/MC/29061-97/C0776

CONF-961105--23

Title:
Measurements in Film Cooling Flows: Hole L/D and Turbulence Intensity Effects

Authors:
S.W. Burd
R.W. Kaszeta
T.W. Simon

Contractor:
University of Minnesota
Department of Mechanical Engineering
111 Church Street SE
Minneapolis, MN 55455-0111

Contract Number:
DE-FC21-92MC29061

Conference:
International Mechanical Engineering Congress and Exposition (IMECE) 1996
International Congress and Exposition

Conference Location:
Atlanta, Georgia

Conference Dates:
November 17-22, 1996

Conference Sponsor:
International Mechanical Engineering Congress and Exposition

Disclaimer

Gas Turbine Heat Transfer Session
1996 IMECE Conference
Atlanta, GA

MEASUREMENTS IN FILM COOLING FLOWS:

HOLE L/D AND TURBULENCE INTENSITY EFFECTS

Steven W. Burd, Richard W. Kaszeta, and Terrence W. Simon

Heat Transfer Laboratory
University of Minnesota
Minneapolis, MN 55455, U.S.A.

ABSTRACT

Hot-wire anemometry measurements of simulated film cooling are presented to document the influence of the freestream turbulence intensity and film cooling hole length-to-diameter ratio on mean velocity and on turbulence intensity. Measurements are taken in the zone where the coolant and freestream flows mix. Flow from one row of film cooling holes with a streamwise injection of 35° and no lateral injection and with a coolant-to-freestream flow velocity ratio of 1.0 is investigated under freestream turbulence levels of 0.5% and 12%. The coolant-to-freestream density ratio is unity. Two length-to-diameter ratios for the film cooling holes, 2.3 and 7.0, are tested. The measurements document that under low freestream turbulence conditions, pronounced differences exist in the flowfield between L/D=7.0 and 2.3. The differences between L/D cases are less prominent at high freestream turbulence intensities. Generally, short-L/D injection results in "jetting" of the coolant farther into the freestream flow and enhanced mixing. Other changes in the flowfield attributable to a rise in freestream turbulence intensity to engine-representative conditions are documented.

NOMENCLATURE

D	diameter of the film cooling holes
DR	density ratio
FSTI	freestream turbulence intensity
L	length of the film cooling delivery tube
Re_D	Reynolds number based on mean film cooling hole velocity and hole diameter
Re_θ	Reynolds number based on mean streamwise velocity and momentum thickness
TI	local turbulence intensity normalized with local mean streamwise velocity (u_{rms}/U)
U	time average local streamwise velocity
U_{hole}	mean velocity of coolant flow through film cooling hole
U_o	time average freestream velocity
u'	instantaneous values of streamwise velocity fluctuations
u_{rms}	rms fluctuation of streamwise velocity ($\sqrt{\overline{u'^2}}$)
VR	ratio of film coolant mean velocity to freestream velocity
x	streamwise distance from center of the hole
y	distance normal to the test wall
z	lateral/spanwise distance from center of the middle hole

Greek:

θ	momentum thickness
δ	boundary layer thickness (99%)
δ^*	displacement thickness
ε	eddy diffusivity

Subscripts:

A-F	test case designation
M	momentum

Superscripts:

$\overline{\ }$	time-averaged

INTRODUCTION

Film cooling is commonly used to avert distress and failure of turbine blades in gas turbine engines resulting from excessive operating temperatures. In film cooling, cool air is bled from the compressor stage, ducted to the internal chambers of the turbine blades, and discharged through small holes in the blade walls. This

air provides a thin, cool, insulating blanket along the external surface of the turbine blade. The cooling effectiveness is dependent upon the approach flow turbulence; the film cooling flow temperature, velocity distribution, and turbulence; and the blade and film cooling hole geometries.

Film cooling literature is extensive. It concentrates primarily on surface and flowfield measurements. Surface measurements include film cooling effectiveness and heat transfer coefficient measurements whereas flowfield measurements include mean velocity and turbulence intensity distributions and turbulent shear stress. Computational studies have shown advancements in algorithms, grid flexibility, and turbulence modeling. Continued modeling success, though, relies on experimental support.

Surface and flowfield measurements in the literature exist for slot, transpiration, and single- or multiple-row injection configurations. Surface measurements are presented by Goldstein et al. (1968), Pedersen et al. (1977), Foster and Lampard (1980), and Forth and Jones (1988). Flowfield measurements include pitot probe mapping by Le Brocq et al. (1973) and Foster and Lampard (1980). Crabb et al. (1981) studied the hydrodynamics of a normal jet of L/D=30 in crossflow using hot-wires in the far field and laser Doppler velocimetry in the near field. Andreopoulos and Rodi (1984) investigated the turbulence field for a normal jet in crossflow with L/D=12, DR=1.0, and VR=0.5. They documented (1) skewing of the velocity towards the downstream edge of the hole exit and (2) flow disturbances created by the jet-crossflow interaction upstream of the hole exit and within the jet supply. Inclined jets were studied by Launder and York (1974), Kadotani and Goldstein (1979), Yoshida and Goldstein (1984), and Jubran and Brown (1985). Lee et al. (1992) presented three-dimensional mean velocity and vorticity distributions, accompanied by flow visualization, for 35°-inclined streamwise injection with L/D=50 and freestream turbulence intensity (FSTI) of 0.2%. They showed that a pair of bound vortices accompanied with a complex three-dimensional flow exists downstream of the jet exit, as with normal injection. All these studies were with large length-to-diameter ratios (ranging from 10 to 62), atypical of gas turbines. The benefit of a long L/D was that a fully-developed, turbulent velocity exit profile was achieved. Goldstein et al. (1974) found no appreciable difference in effectiveness between an L/D=5.2 and long injection lengths. Thus, the investigations of Jumper et al. (1991) (L/D=6) and Ligrani et al. (1994) (L/D=8) are in the long-L/D category.

Other researchers have elected to use shorter length-to-diameter ratios which are more representative of turbines. Sinha et al. (1991) used a length-to-diameter ratio of 1.75 while Sen et al. (1994) and Schmidt et al. (1994) used L/D=4. Similarly, L/D=3.5 was used by Bons et al. (1994) and Pietrzyk et al. (1989, 1990) for studies of 35° streamwise injection.

The majority of the above cases were conducted with FSTI <1%. Launder and York (1974) found no influence of 4% FSTI. Brown and Saluja (1979) and Brown and Minty (1975) found losses in cooling effectiveness for FSTI ranging from 2 to 8%. Bons et al. (1994) documented film cooling effectiveness with FSTI=0.9%, 6.5%, 12%, and 17.5%, several velocity ratios, and L/D=3.5. High FSTI enhanced mixing, reduced film cooling effectiveness (by up to 70%) in the region directly downstream of the injection hole, and increased film cooling effectiveness 50-100% in the near-hole regions between holes. Flowfield measurements were presented by MacMullin et al. (1989) for FSTI in the range of 7 to 18%. Gogineni et al. (1996) used two-color particle image velocimetry to investigate velocity and vorticity fields in 35°, single-row injection with FSTI values from 1 to 17%. Wang et al. (1996) used three-wire anemometry to document the flowfield just downstream of injection for FSTI=0.5% and 12%. Computed from the data were the eddy diffusivities in the lateral direction, $\varepsilon_{M,z}$, and wall-normal directions, $\varepsilon_{M,y}$, and the ratio of the two. This ratio documents the anisotropy of turbulent transport.

These studies demonstrate that film cooling is strongly dependent upon the FSTI. Measurements of combustor exit flows by Goebel et al. (1993) document levels of 8-12%.

Computation includes a two-dimensional, parabolic model with low-Reynolds-number, k-ε turbulence by Tafti and Yavuzkurt (1988) and three-dimensional computations by Patankar and Spalding (1972) and Patankar et al. (1973). Bergeles et al. (1976 and 1978) used the partially-parabolic, three-dimensional procedure of Pratap and Spalding (1976) to predict discrete-hole cooling performance. Demuren and Rodi (1983) applied the locally-elliptic procedure of Rodi and Srivatsa (1980) to allow computation at high blowing rates and later extended the study (Demuren et al. 1986). Leylek and Zerkle (1994) performed three-dimensional, Navier-Stokes computation and compared their results to the experiments of Pietrzyk et al. (1989, 1990) and Sinha et al. (1991). They found that film cooling exit flow includes counter-rotating vortices and local jetting effects. They suggested that film cooling experiments with long L/D may be misleading. The above computational works were performed using the k-ε, two-equation turbulence model to estimate the Reynolds stress terms in the time-averaged momentum equations. Most computations assumed isotropy in that lateral eddy diffusivity was set equal to wall-normal eddy diffusivity. This was found to be unsatisfactory by Sathyamurthy and Patankar (1990). They showed improvements with a modification proposed by Bergeles et al. (1978). Wang et al. (1996) measured larger anisotropy than given by the Bergeles et al. modification. Recent computations at the University of Minnesota show further improvement with the Wang et al. values.

Over the years, researchers have restricted their test cases to a limited number of film cooling parameters. Although each has contributed to general understanding, differences in test and flow configurations make comparing results of one with another difficult. Specifically, no direct comparisons of the roles of L/D and turbulence intensity can be clearly made for they were often conducted in separate facilities and under different conditions. In this paper, the results of an experimental study of the effects of both the film cooling hole length-to-diameter ratio and FSTI on the flowfield zone where the coolant and freestream flows mix are presented, all from a common facility. Mean velocity and local turbulence intensity distributions are presented for planes that are normal to the flow at x/D=2.5 downstream of injection and measurements at x/D=5.0 are discussed. Two L/D values and two FSTI levels, with VR=1.0, are presented. The focus of the current program is on differences between long and short L/D delivery and between low and high FSTI.

EXPERIMENTAL TEST FACILITY

High-turbulence Freestream Facility

The high-turbulence freestream facility is a small, blown-type wind tunnel which simulates the flow of a gas turbine combustor. The facility is described by Wang et al. (1996). The measured freestream turbulence is nearly isotropic at the 68.6cm x 12.7cm nozzle exit (Fig. 1) with an intensity 12%, a level characteristic of flow exiting the combustor stage in actual gas turbine engines (Goebel et al. 1993). The exit-plane turbulence intensity and mean velocity are uniform to within 2% of their mean values and the integral length scale calculated from a u' power spectrum is 3.3 cm.

Low-turbulence Freestream Facility

The low turbulence freestream facility is also a blown-type wind tunnel. This is a standard configuration with a fan, screens, a setting chamber, and a 6.4:1 area-reduction nozzle of exit area 68.6cm x 12.7cm (Fig. 1). Measured turbulence intensity is 0.5%. Mean velocity is uniform within 2% over the core of the nozzle exit.

Test Section

The test section (Fig. 1) consists of an upstream plate (25.4 cm x 68.6 cm), the test plate (15.2 cm x 68.6 cm), a downstream plate (91 cm x 68.6 cm), and the film coolant supply system. There is a single column of eleven film cooling holes distributed uniformly across the test plate. Film cooling flow is injected at an angle of 35° in the streamwise direction with the film cooling holes machined to a diameter of 1.9 cm and positioned three diameters apart, center-to- center. The film cooling delivery tubes have length-to-diameter ratios of 7 and 2.3. The larger establishes fully-developed flow within the delivery tube (Goldstein et al. 1974). The smaller represents film cooling designs in modern airfoils. A square-edged, rectangular polycarbonate strip (1.6 mm thick x 13 mm wide x 68.6 cm long) is attached to the upstream plate as a boundary layer trip. Its upstream edge is 21.1 cm upstream of the hole centers. Film cooling flow is supplied by a fan through a metering section and a large, unrestricted supply plenum. The supply system is designed for uniform distribution of flow to the holes. The metering section is fabricated with two laminar-type flow meters.

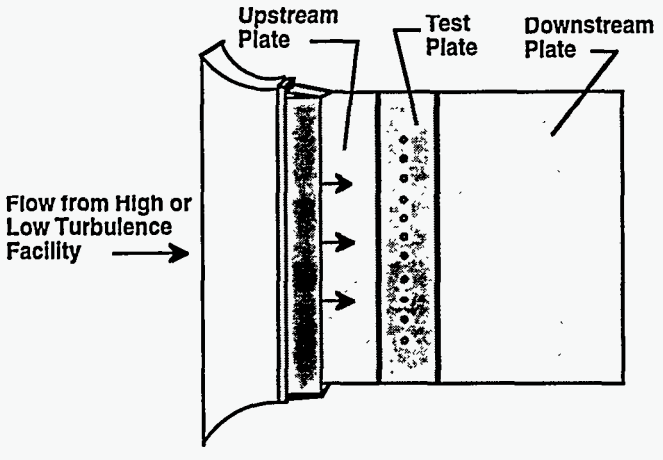

Figure 1: Test Section

Table 1 and Fig. 2 document the approach flows. The coolant has Re_D=13,000 to achieve a velocity ratio of 1.0. The coolant-to-freestream density ratio is unity.

Table 1: Approach Flow

			x/D=-4.0				x/D=0#
	U_o (m/s)	FSTI	δ/D	θ/D	δ*/D	Re_θ	Re_θ
Low FSTI	10.8	0.5	0.52	0.05	0.073	655	750
High FSTI	10.8	12	1.10	0.073	0.094	960	1075

Projected with turbulent boundary layer growth rate

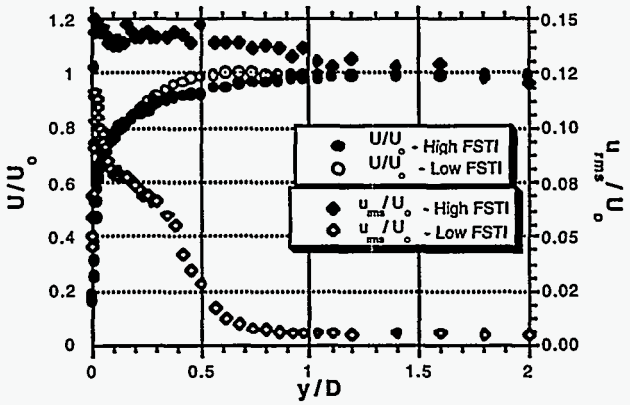

Figure 2: Velocity and Turbulence Intensity Profiles of the Approach Flow (Measurement Location: x/D=-4.0)

Instrumentation

Single-sensor (TSI model 1218-T1.5) hot-wire probes are used to obtain the velocity and turbulence data. They are driven by a TSI IFA-100 bridge unit. A total of 4096 data points was recorded for each measurement location over a sampling time of 40 seconds. Hot-wire measurements are suitable for they are made in regions where there is no recirculating flow and local turbulence intensities are sufficiently low.

An automated, two-dimensional traversing system allowed high-spatial-resolution (0.025 mm capability) measurements in the

wall-normal and spanwise directions. Movement in the streamwise direction was accomplished manually.

Experimental Uncertainty

Hot-wire uncertainty comes from precision and bias error. Such uncertainties, which arise during calibration and measurement, are larger at smaller velocities. They result from items such as changes in fluid properties between calibration and measurement, near-wall effects, and sensor drift. A standard propagation of uncertainties, as detailed by Kline and McClintock (1953), yields a combined uncertainty of 7% (~3 m/s) to 5% (~10 m/s). Due to the large sample sizes and long sampling time associated with the hot-wire calibration and measurement, stochastic errors associated with sampling size and time fall well below the deterministic errors and are negligible in comparison. The rms velocity fluctuation and the mean velocity have the same uncertainty.

Comparisons of mean velocity and turbulence intensity to data by Laufer (1953) in a fully-developed pipe are used to corroborate these computed values. Per this data, bias error contributions on the order of 5% of mean values are reasonable under the conditions of the bulk of the present data, so long as velocity fluctuation rms levels remain below 25% of the mean streamwise velocity. Our uncertainties are consistent with previous experience with such measurements and with Yavuzkurt (1984). Uncertainty in the total coolant mass flow rate is 2.3%. All uncertainties are expressed with 95% confidence.

Cases Studied

Surveys were taken at the two planes shown in Fig. 3. Data are taken in the lateral direction at fourteen evenly spaced locations. The extrema of these locations are z/D=-0.5 and z/D=1.67. Data are distributed in the wall-normal direction with high-resolution (y/D=0.0025) in the near-wall region and with a gradual transition to coarser resolution (y/D=0.3) in the freestream. All measurements were taken about the middle hole of the eleven film cooling holes. Cases with different hole length-to-diameter ratios, FSTI values, and streamwise positions are documented in Table 2.

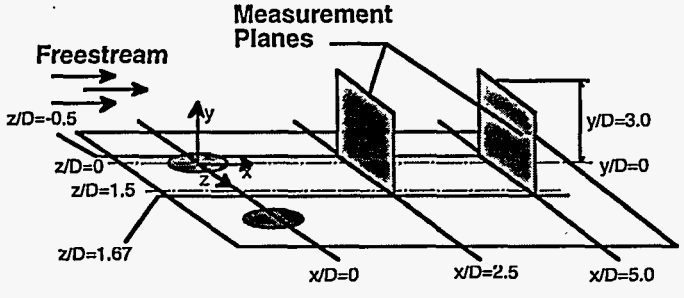

Figure 3: Streamwise-Normal Measurement Planes

Table 2: Cases in this Study

CASE	L/D	FSTI	VR	x/D
A	7.0	0.5%	1.0	2.5
B	2.3	0.5%	1.0	2.5
C	7.0	0.5%	1.0	5.0
D	2.3	0.5%	1.0	5.0
E	7.0	12%	1.0	2.5
F	2.3	12%	1.0	2.5

EXPERIMENTAL RESULTS

To separate effects, results are presented in three sections. The first highlights the influence of the hole length-to-diameter ratio with FSTI=0.5%. The second documents the effects of the hole length-to-diameter ratio with FSTI=12%. The third explores the effects of FSTI with a fixed geometry. It will be shown that both the hole length-to-diameter ratio and FSTI play influential roles.

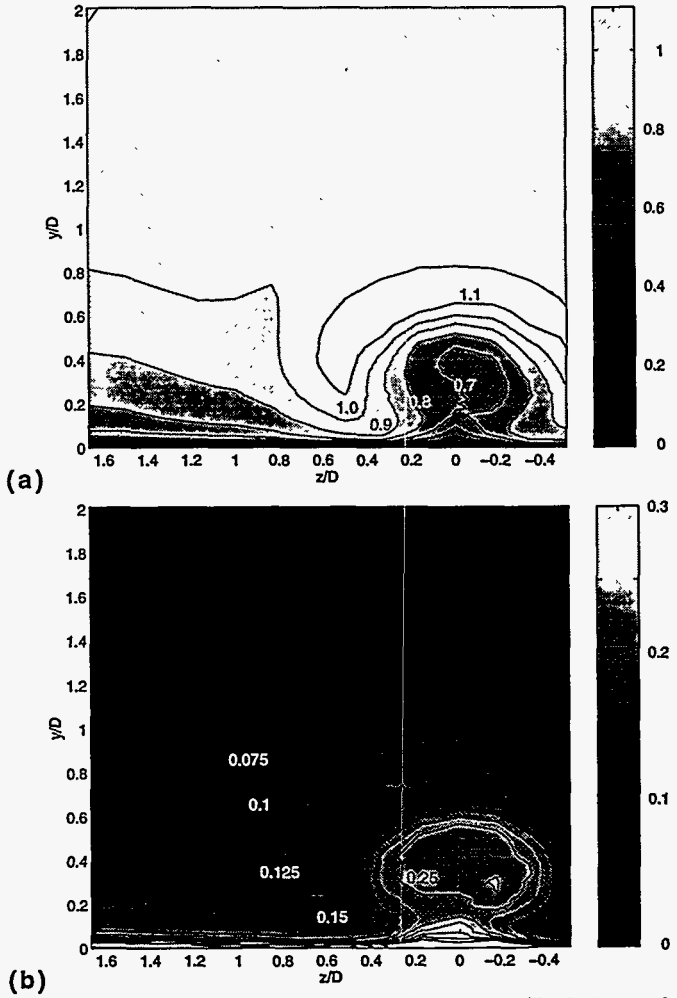

Figure 4: Case A - L/D=7.0, VR=1.0, x/D=2.5, and FSTI=0.5% (a) U/U_o (b) TI

Figures 4(a) and 4(b) show contour plots of the normalized mean velocity (U/U_o) and local turbulence intensity (TI), respectively, for Case A (L/D=7.0, 0.5% FSTI) and Figs. 5(a) and 5(b) are for Case E (L/D=7.0, 12% FSTI). These cases will serve as base cases for comparison. In the proceeding sections, the "core" refers to the center of the region influenced by the coolant flow in which velocity gradients are small. The "mixing region" refers to the coolant jet periphery in which velocity gradients are large.

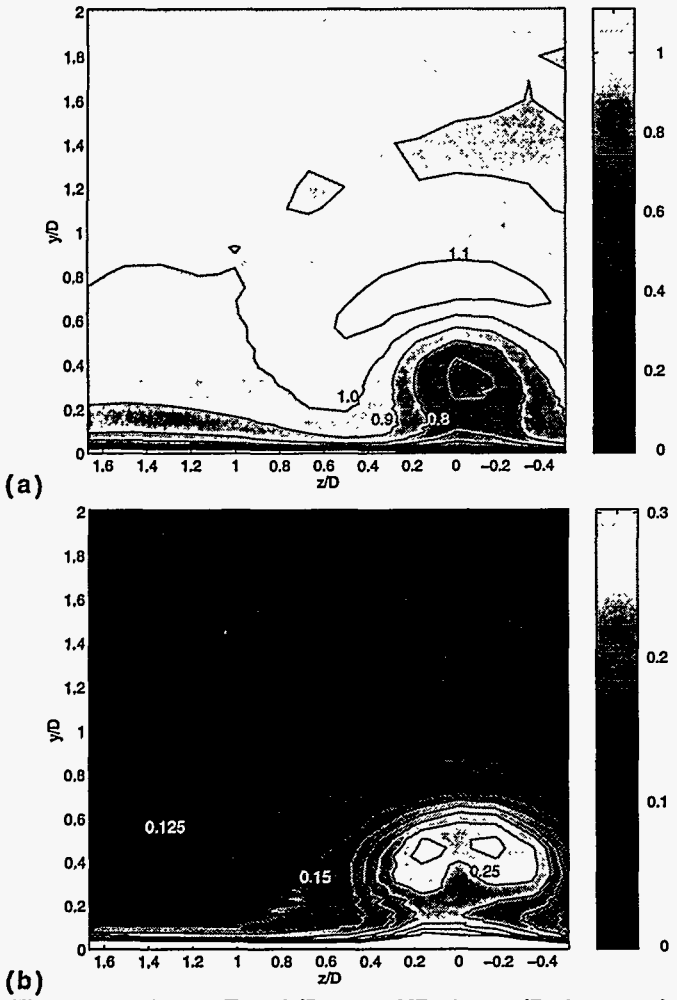

Figure 5: Case E - L/D=7.0, VR=1.0, x/D=2.5, and FSTI=12.0% (a) U/U_o (b) TI

L/D Influence at Low FSTI

This section documents the hole L/D effect by comparing case A to case B. Pietrzyk et al. (1989, 1990) and Leylek and Zerkle (1994) recorded a strong effect of L/D, noting that short-hole injection is subject to "jetting" effects. With jetting, the jet velocity profile is not uniformly distributed across the majority of the plane at which it exits, but is skewed with substantially higher velocities upstream (Fig. 6). Although the data presented in Fig. 6 are for high FSTI, Leylek and Zerkle describe similar profiles for low FSTI. Figure 7(a) shows, at x/D=2.5, the percent rise in mean velocity (U/U_o) and Fig. 7(b) shows the rise in TI in going from L/D=7.0 (Case A) to L/D=2.3 (Case B). A rise in the normalized velocity is observed over the majority of the region defined by y/D<0.2 and -0.4<z/D<0.4 in going to the shorter delivery length. The flow emerging from the shorter hole is able to penetrate farther into the freestream flow and accelerates the freestream in that

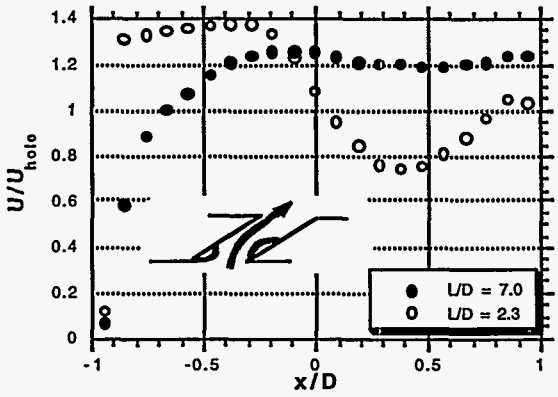

Figure 6: Centerline Mean Velocity Profiles at the Hole-Exit Plane: FSTI=12% (Case E and Case F)

region. With the short-hole injection, the film coolant ejects further into the freestream in the wall-normal direction and spreads more in the spanwise direction, as evidenced by the rise in U/U_o and TI at y/D~0.5 and z/D=±0.6. Enhanced mixing by this type of "jetting" was discussed by Leylek and Zerkle (1994). Negative velocity difference values (Fig. 7(a)) in the zone y/D=0.05 and z/D=±0.3 show a weaker downwash associated with a less coherent jet and a more elevated trajectory of the coolant in the short L/D case. The effects on the local turbulence intensity differences (Fig. 7(b)) are also pronounced, showing that mixing occurs further into the freestream with short-hole injection —note 5% higher values for the short hole case directly downstream of the film cooling holes (z/D=0) at y/D~0.7. In addition, higher turbulence levels extend into the region between the holes, to as far as z/D=0.7, emphasizing the jet lateral spreading. The region of negative TI differences with a change to short L/D holes (y/D~0.3, z/D~0) highlights the higher centerline momentum associated with short-hole injection.

Measurements were taken also at a downstream location, x/D=5.0, Cases C and D. Here, differences between the short-hole and long-hole injection are similar, but reduced.

L/D Influence at High FSTI

This section documents the role of L/D when the FSTI is elevated to combustor exit levels (~12%). Contour plots showing the normalized mean velocity ratio (U/U_o) and local turbulence intensity (TI) distributions are given for Case F (high FSTI, short-L/D case) in Figs. 8(a) and 8(b). This case is most representative of the engine. The role of L/D, with high FSTI, is shown by comparing Cases E and F, as done in Fig. 9. Centerline hole-exit

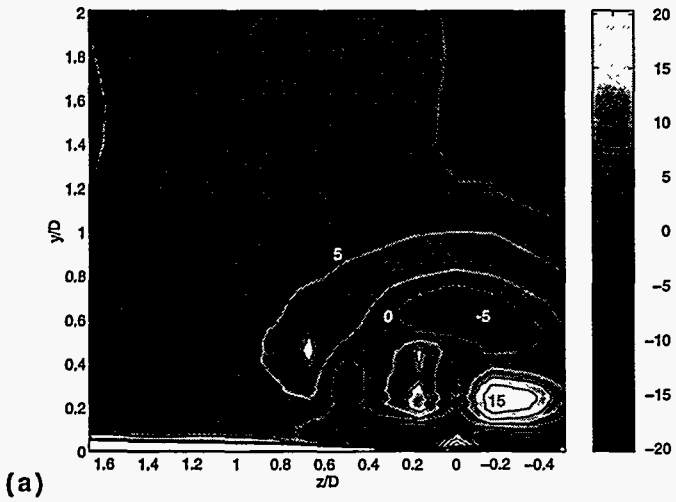

(a)

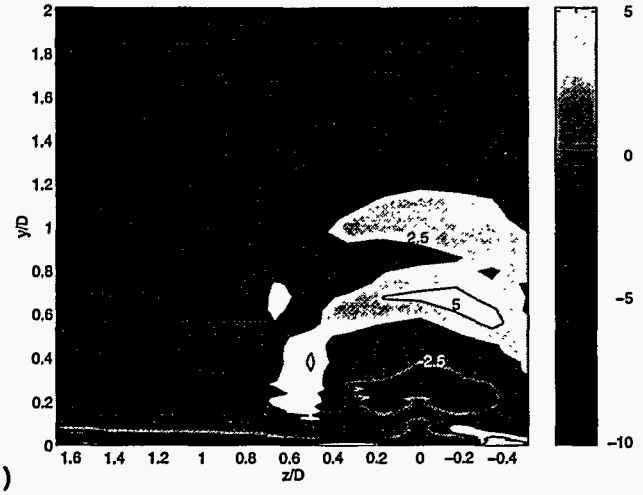

(b)

Figure 7: Case A (L/D=7.0) vs. Case B (L/D=2.3) (a) Percent Change in Mean Velocity Ratio

$$\left[\frac{(U/U_o)_B}{(U/U_o)_A} - 1\right] x100$$

(b) Percent Differences in Local Turbulence

$$(TI_B - TI_A) x100$$

profiles are given for these cases in Fig. 6. There remains a region downstream of the hole centerline (0.2<y/D<0.5 and -0.3<z/D<0.3) where the mean velocities of the short L/D case are higher, indicating the penetration or "jetting" of the low-L/D jet further into the flow. This is similar to the low-FSTI case comparison (Fig. 7(a)). Also, consistent the low-FSTI comparison, negative velocity differences in the zone y/D=0.05 and about z/D=±0.3 show a weaker downwash associated with the less coherent jet and the more elevated trajectory of the short-L/D case. Negative values of percent turbulence intensity difference (Fig. 9(b)) in the zone given by y/D<0.4 along the jet centerline are attributable to the higher momentum of the short hole jet and the associated reduction of shear with the mainstream flow in this region.

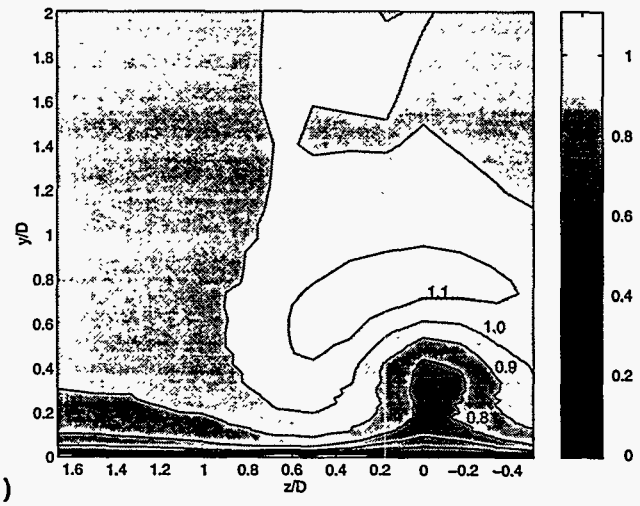

(a)

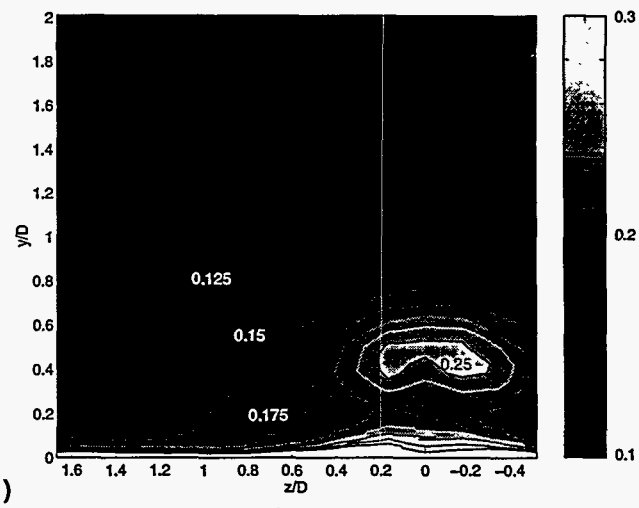

(b)

Figure 8: Case F - L/D=2.3, VR=1.0, x/D=2.5, and FSTI=12.0% (a) U/U_o (b) TI

FSTI Effects

With elevated FSTI, film coolant rapidly mixes with the freestream flow. With this, the film cooling jets diffuse more rapidly, resulting in a dispersed film cooling jet with less influence distant from the wall. In the following section, comparisons at two FSTI levels for the long-hole injection cases (Cases A and E) and the short-hole cases (Cases B and F) are given.

With long L/D, the normalized mean velocity distributions have significant differences. Figure 10 shows the change in mean velocity ratios when changing from the low-turbulence case to the high-turbulence case. First, in the region (0.3<y/D<0.5 and z/D=±0.5), the high-FSTI case has lower mean velocities. This indicates a less coherent structure and more mixing with elevated FSTI in this region. Along the centerline (z/D~0, y/D<0.5), however, the mean velocities are larger for the high-FSTI case, indicating that jetting in this region is more pronounced. Deceleration along the outer portions of this region, caused by the

larger shear in this region, assists with accelerating the jet core. Figure 11 shows u_{rms} contours for the low-FSTI case and Fig. 12 shows u_{rms} contours for the high-FSTI case. Their turbulence structures are similar, with distinct regions detailing the core and mixing regions of the jets. The low-FSTI case shows coolant penetrating further from the wall (to y/D~1.0 along the centerline but to only y/D~0.8 for the high-FSTI case). Consistent with this is a slightly wider lateral (larger z/D) influence of the low-FSTI jet (see Fig. 11). Elevated u_{rms} levels extend to z/D~0.8 for the high-FSTI case and to z/D~1.0 for the low-FSTI case.

The same comparison of different FSTI cases is made for short-L/D injection. Changes in mean velocity ratios in going to high FSTI are noted in Fig. 13. Although generally the regions of

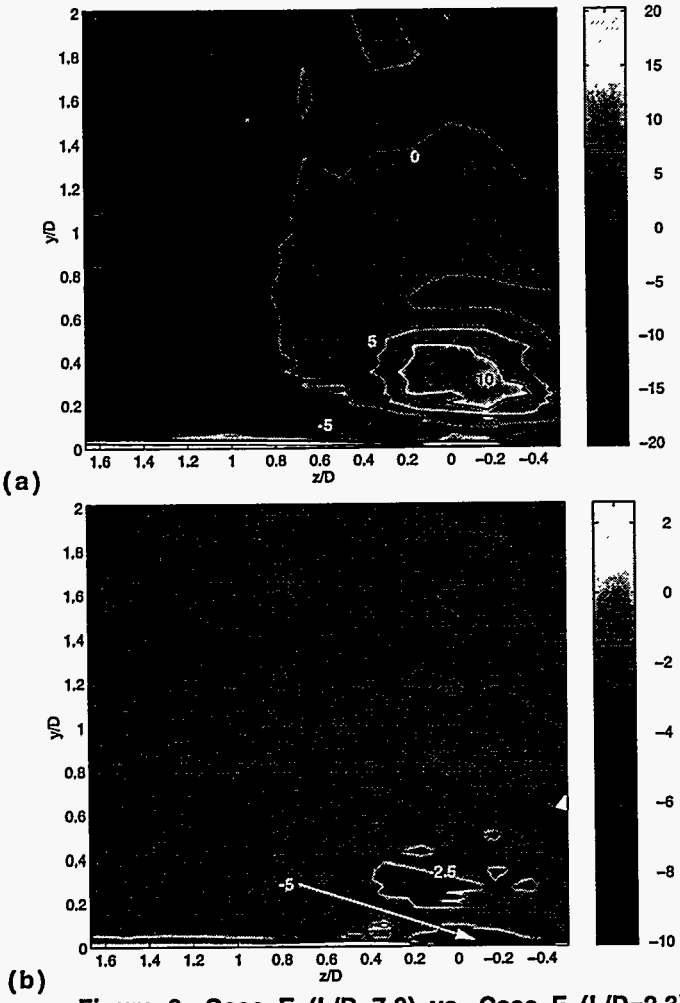

Figure 9: Case E (L/D=7.0) vs. Case F (L/D=2.3)
(a) Percent Change in Mean Velocity Ratio

$$\left[\frac{(U/U_o)_F}{(U/U_o)_E}-1\right]x100$$

(b) Percent Differences in Local Turbulence
$(TI_F-TI_E)x100$

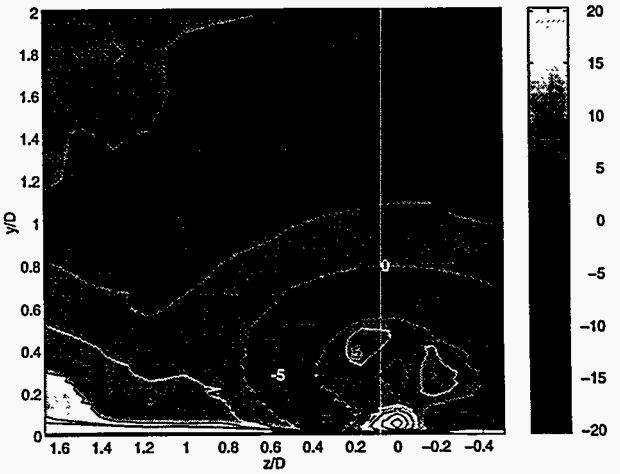

Figure 10: Percent Change in Mean Velocity Ratio, Case E (FSTI=12%) vs. Case A (FSTI=0.5%)

$$\left[\frac{(U/U_o)_E}{(U/U_o)_A}-1\right]x100$$

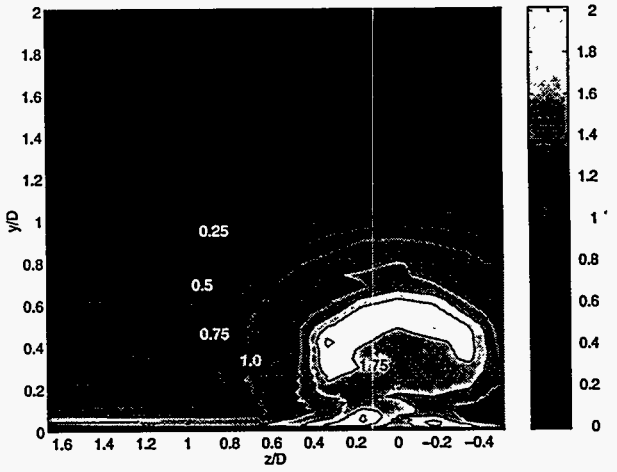

Figure 11: u_{rms} (m/s) Distribution for Case A (FSTI=0.5%, L/D=7.0)

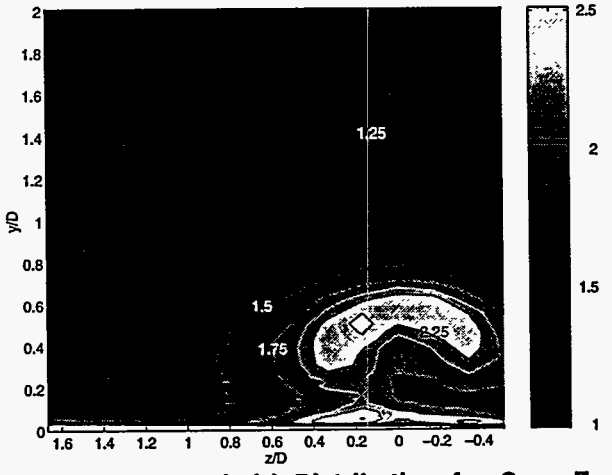

Figure 12: u_{rms} (m/s) Distribution for Case E (FSTI=12%, L/D=7.0)

difference are shared with the long-L/D case, the magnitudes are changed. The low-FSTI case maintains higher mean velocities along the outer edges of the jets (y/D~0.3-0.7 and z/D=0.6). Differences in this outer region extend to z/D~0.8, farther in the spanwise direction than those found with the long-L/D comparison case. This indicates that in the high-FSTI case, the jet is decelerating and mixing to a greater extent than in the low-FSTI case. About the hole centerline (-0.4<z/D<0.4 and y/D<0.6), mean velocities are higher for the high-FSTI case. This again shows that the high-FSTI case has enhanced jetting in the jet core region, primarily due to more deceleration and shearing along the periphery of the jet. A comparison of u_{rms} distributions (Figs. 14, for the low-FSTI case, and 15, for high-FSTI) shows an influence of the jets in both cases which extends to y/D~1 for high FSTI and to y/D~1.15 for low FSTI. A somewhat wider influence of the jets laterally for the low-FSTI case is also apparent.

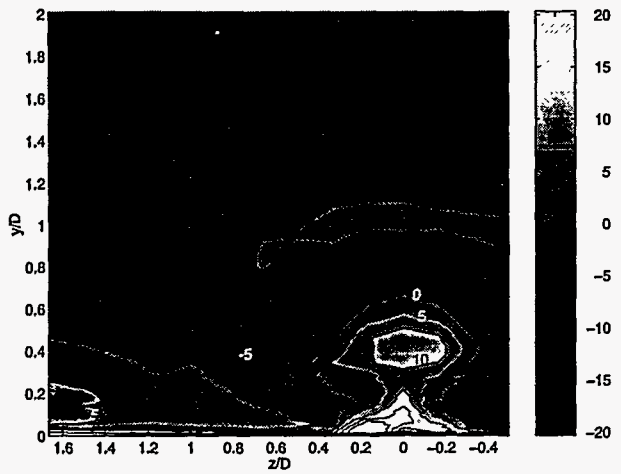

Figure 13: Percent Change in Mean Velocity Ratio - Case F (FSTI=12%) vs. Case B (FSTI=0.5%)

$$\left[\frac{(U/U_o)_F}{(U/U_o)_B} - 1\right] x100$$

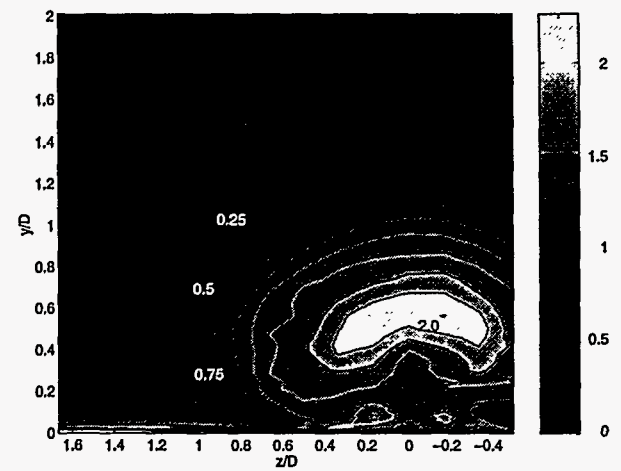

Figure 14: u_{rms} (m/s) Distribution for Case B (FSTI=0.5%, L/D=2.3)

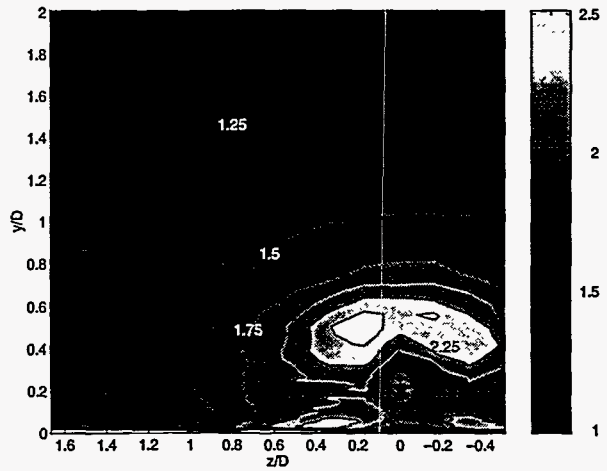

Figure 15: u_{rms} (m/s) Distribution for Case F (FSTI=12%, L/D=2.3)

CONCLUDING REMARKS

The comparisons emphasize that L/D and FSTI play influential roles in film cooling. We also note a cross-correlation of these two effects which makes interpretation of one in isolation of the other incomplete. Film cooling with low FSTI is more affected by changes in L/D than that with high FSTI and, as a result, shows significant differences between the L/D=7.0 and L/D=2.3 cases. High-FSTI film cooling shows a lesser difference between L/D cases, but many of the same trends. Details are:

- Under low-FSTI conditions, the short-hole injection flow penetrates further from the wall and influences a greater extent of the region downstream from the hole. The long-hole injection interacts significantly less. With a low FSTI, the short-hole jet is observed to influence the flow more in the spanwise direction and have a more pronounced acceleration and shearing along the jet periphery.
- With high FSTI, jetting effects and higher jet core velocities are associated with short-L/D injection. Long-L/D injection appears to have a more coherent jet structure. No significant differences in normalized mean velocities and TI are seen in the region between the holes.
- Comparing like geometries under differing FSTI conditions yields turbulent structures that are generally similar but shows signs of significant differences in mixing and penetration. In general, high-FSTI cases are more influenced by the freestream and are characterized by increased mixing downstream of the edges of the film cooling holes.

ACKNOWLEDGMENTS

This work is part of a combined study of film cooling with short-hole delivery holes and with lateral injection sponsored by NASA-Lewis Research Center and DOE, respectively. The DOE project is managed by Dr. Daniel Fant of the South Carolina Energy

R&D Center and the NASA study Project Monitor is Douglas Thurman. The authors would also like to acknowledge Dr. E.R.G. Eckert for his invaluable contributions to this work.

REFERENCES

Andreopoulos, J. and Rodi, W., 1984, "Experimental Investigation of Jets in a Crossflow," J. Fluid Mechanics, Vol. 138, pp. 93-127.

Bergeles, G., Gosman, A. D., and Launder, B. E., 1976, "The Prediction of Three-Dimensional Discrete-Hole Cooling Processes, Part 1 - Laminar Flow," ASME J. Heat Transfer, Vol. 98, No. 3, p. 379.

Bergeles, G., Gosman, A. D., and Launder, B. E., 1978, "The Turbulent Jet in a Cross Stream at Low Injection Rates: A Three-Dimensional Numerical Treatment," Num. Heat Transfer, Part A: Applications, Vol. 1, pp. 217-242.

Bons, J. P., MacArthur, C. D., and Rivir, R. B., 1994, "The Effect of High Freestream Turbulence of Film Cooling Effectiveness," ASME Paper 94-GT-51.

Brown, A. and Minty, A. G., 1975, "The Effects of Mainstream Turbulence Intensity and Pressure Gradient on Film Cooling Effectiveness for Cold Air Injection Slits of Various Ratios," ASME Paper 75-WA/HT-17.

Brown, A. and Saluja, C. A., 1979, "Film Cooling from Three Rows of Holes on an Adiabatic Constant Heat Flux and Isothermal Surfaces in the Presence of Variable Free-Stream Velocity Gradients and Turbulence Intensity," ASME Paper 79-GT-24.

Crabb, D., Durao, D. F. G., and Whitelaw, J. H., 1981, "A Round Jet Normal to a Crossflow," ASME J. Fluids Engineering, Vol. 103, pp. 1006-1012.

Demuren, A. O. and Rodi, W., 1983, "Three-Dimensional Calculation of Film Cooling by a Row of Jets," Notes Num. Fluid Mech., Vol. 7, p. 49-56.

Demuren, A. O., Rodi, W., and Schonung, B., 1986, "Systematic Study of Film Cooling With a Three-Dimensional Calculation Procedure, " ASME J. of Turbomachinery, Vol. 108, pp. 124-130.

Forth, C. J. P. and Jones, T. V., 1988, "Scaling Parameters in Film Cooling," Proc. 8th Int. Heat Transfer Conference, Vol. 3, pp. 1271-1276.

Foster, N. W. and Lampard, D., 1980, "The Flow and Film Cooling Effectiveness Following Injection Through a Row of Holes," ASME J. Engineering for Power, Vol. 102, pp. 584-588.

Goldstein, R. J., Eckert, E. R. G., and Burggraf, F., 1974, "Effects of Hole Geometry and Density on Three-Dimensional Film Cooling," Int. J. Heat Mass Transfer, Vol. 17, pp. 595-607.

Goldstein, R. J., Eckert, E. R. G., and Ramsey, J. W., 1968, "Film Cooling with Injection Through Holes: Adiabatic Wall Temperatures Downstream of a Circular Hole," ASME J. Engineering for Power, pp. 384-395.

Goebel, S. G., Abuaf, N., Lovett, J. A., and Lee, C.-P., 1993, "Measurements of Combustor Velocity and Turbulence Profiles," ASME Paper 93-GT-228.

Gogineni, S. P., Rivir, R. B., Pestian, D. J., and Goss, L. P., 1996, "PIV Measurements of Flat Plate Film Cooling Flow with High Free Stream Turbulence," AIAA Paper 96-0617.

Jubran, B. and Brown, A., 1985, "Film Cooling from Two Rows of Holes Inclined in the Streamwise and Spanwise Directions," ASME J. of Engineering for Gas Turbine and Power, Vol. 107, pp. 84-91.

Jumper, G. W., Elrod, W. C., and Rivir, R. B., 1991, "Film Cooling Effectiveness in High-Turbulence Flow," ASME J. Turbomachinery, Vol. 113, pp. 479-483.

Kadotani, K. and Goldstein, R. J., 1979, "On the Nature of Jets Entering a Turbulent Flow, Part A: Jet-Mainstream Interaction," ASME J. Engineering for Power, Vol. 101, pp. 459-465.

Kline, S. J. and McClintock, F. A., 1953, "Describing Uncertainties in Single-sample Experiments, Mechanical Eng., January, pp. 3-8.

Laufer, J., 1953," The Structure of Turbulence in Fully-Developed Pipe Flow," NACA Report 1174.

Launder, B. E. and York, J., 1974, "Discrete-Hole Cooling in the Presence of Free Stream Turbulence and Strong Favorable Pressure Gradients," Int. J. Heat Mass Transfer, Vol. 17, pp. 1403-1409.

Le Brocq, P. V., Launder, B. E., and Priddin, C. H., 1973, "Discrete Hole Injection as a Means of Transpiration Cooling: An Experimental Study," Proc. Inst. Mech. Eng., Vol. 187, pp. 149-157.

Lee, S. W., Lee, J. S., and Ro, S. T., 1992, "Experimental Study of the Flow Characteristics of Streamwise Inclined Jets in Crossflow on Flat Plate," ASME Paper 92-GT-181.

Leylek J. H. and Zerkle R. D., 1994, "Discrete-Jet Film Cooling: A Comparison of Computational Results with Experiments," ASME J. Turbomachinery, Vol. 116, pp. 358-368.

Ligrani, P. M., Wigle, J. M., Ciriello, S., and Jackson, S. M., 1994, "Film Cooling from Holes with Compound Angle Orientations, Part 1: Results Downstream of Two Staggered Rows of Holes with 3d Spanwise Spacing," ASME J. Heat Transfer, Vol. 116, pp. 341-352.

MacMullin, R., Elrod, W. C., and Rivir, R. B., 1989, "Free Stream Turbulence from a Circular Wall Jet on Flat Plate Heat Transfer and Boundary Layer Flow," ASME J. Turbomachinery, Vol. 111, pp. 78-86.

Patankar, S. V. and Spalding, D. B., 1972, "A Calculation Procedure for Heat, Mass and Momentum Transfer in Three-Dimensional Parabolic Flows," Int. J. Heat Mass Transfer, Vol. 15, p. 1787.

Patankar, S. V., Rastogi, A. K., and Whitelaw, J. H., 1973, "The Effectiveness of Three-Dimensional Film-Cooling Slots - II. Predictions," Int. J. Heat Mass Transfer, Vol. 16, pp. 1665-1681.

Pedersen, D. B., Eckert, E. R. G., and Goldstein, R. J., 1977, "Film Cooling with Large Density Differences Between the Mainstream and Secondary Fluid Measured by Heat-Mass Transfer Analogy," ASME J. Heat Transfer, Vol. 99, pp. 620-627.

Pietrzyk, J. R., Bogard, D. G., and Crawford, M. E., 1989, "Hydrodynamic Measurements of Jets in a Crossflow for Gas Turbine Film Cooling Applications," ASME J. Turbomachinery, Vol. 111, pp. 139-145.

Pietrzyk, J. R., Bogard, D. G., and Crawford, M. E., 1990, "Effects of Density Ratio on the Hydrodynamics of Film Cooling," ASME J. Turbomachinery, Vol. 112, pp. 437-443.

Pratap, V. S., and Spalding, D. B., 1976, "Fluid Flow and Heat Transfer in Three-Dimensional Duct Flows," Int. J. Heat Mass Transfer, Vol. 19, p. 1183.

Rodi, W. and Srivatsa, S. K., 1980, "A Locally Elliptic Calculation Procedure for Three-Dimensional Flows and Its Application to a Jet in Cross-Flow," Comp. Mech. App. Mech. Eng., Vol. 23, pp. 67-83.

Sathyamurthy, P. and Patankar, S. V., 1990, "Prediction of Film-Cooling with Lateral Injection," Heat Transfer in Turbulent Flows, ASME-HTD, Vol. 138, pp. 61-70.

Schmidt, D. L., Sen, B., and Bogard, D. G., 1994, "Film Cooling with Compound Angle Holes: Adiabatic Effectiveness," ASME paper 94-GT-312.

Sen, B., Schmidt, D. L., and Bogard, D. G., 1994, "Film Cooling with Compound Angle Holes: Heat Transfer," ASME Paper 94-GT-311.

Sinha, A. K., Bogard, D. G., and Crawford, M. E., 1991, "Film Cooling Effectiveness of a Single Row of Holes with Variable Density Ratio," ASME J. Turbomachinery, Vol. 113, pp. 442-449.

Tafti, D. K. and Yavuzkurt, S., 1988, "Prediction of Heat Transfer Characteristics of Discrete Hole Film Cooling - One Row of Injection into a Turbulent Boundary Layer," ASME HTD-Vol. 103, pp. 45-52.

Wang, L., Tsang, H., Simon, T. W., and Eckert, E. R. G., 1996, "Measurements of Mean Flow and Eddy Transport over a Film Cooled Surface," ASME-HTD, Vol. 327, pp. 71-79.

Yavuzkurt, S., 1984, "A Guide to Uncertainty Analysis of Hot-Wire Data," J. Fluids Engineering, June, Vol. 106, pp. 181-186.

Yoshida, T. and Goldstein, R. J., 1984, "On the Nature of Jets Issuing from a Row of Holes into a Low Reynolds Number Mainstream Flow," ASME J. Engineering for Gas Turbines and Power, Vol. 106, pp. 612-618.